Numerical Boltzmann Equation Solutions for Secretly Asymmetric Dark Matter Scenarios

Christopher Dessert

PHY 379H Honors Tutorial Course

Department of Physics

The University of Texas at Austin

Undergraduate Honors Thesis

Supervising Professor: Dr. Can Kilic

Honors Advisor: Dr. Greg Sitz

May 2017

Abstract

Everything that anyone interacts with on a daily basis is made up of ordinary matter: food, the Earth, and ourselves. However, during the 1900s people began to realize that the universe was not purely ordinary matter. When studying the motions of stars in other galaxies, scientists found that the velocity of the stars weren't what one would expect based on Newtonian physics—instead of stellar velocities decreasing as the distance from the center grows, they remain constant [1]. They hypothesized that this discrepancy was a result of a large amount of unseen mass clustered around the galaxies, and dubbed this unseen mass "dark matter." Today, we know that dark

matter must make up about 80% of the matter in the universe, with our ordinary matter the other 20%. We have found a whole host of other evidence for dark matter, including the excess curvature of light around galaxies [2] and the anisotropy of the cosmic microwave background [3]. Nevertheless, we still know very little about the nature of dark matter.

The Standard Model (SM) of particle physics was completed as we know it today in 1967 [4], but experimental confirmation had to wait until 2012 when the Large Hadron Collider (LHC) announced the discovery of the Higgs boson [5]. In the meantime many particle theorists have been searching for physics Beyond the Standard Model (BSM), one part of which is the search for a particle physics explanation of dark matter.

One potential explanation is asymmetric dark matter (ADM) [6], in which the initial amount of dark matter and antidark matter in the universe is unequal. What makes our model, one of several ADM models, special is that there are three flavors, or types, of dark matter and even though the initial amounts are unequal in each flavor, the total amount of dark matter is equal to that of antidark matter. The three flavors interact in various ways. These interactions serve to change the flavor of the dark matter particles or annihilate them altogether. One important interaction is the decay of the heavier flavors into lighter flavors, and after a long time only the light flavor will remain. In this case there will appear to only be one flavor of dark matter with equal amounts of dark matter and antidark matter. For this reason, the model is named "Secretly Asymmetric Dark Matter (SADM) [7]." The results presented in this thesis are a direct followup to this work.

We would like to understand if the model could be a realistic theory for dark matter. To do so, we use the interactions to write down a set of equations, known as Boltzmann equations, that model the density of the dark matter in the early universe as it expands and see if the results match experimental measurements today. The interactions are complicated and the resulting equations are impossible to solve by hand. I have written a program in Mathematica 11 that will solve them numerically.

1 Introduction

Ordinary matter is made up mostly of baryons (including protons and neutrons) and leptons (including electrons). Since baryons are much more massive than leptons, the baryon energy density comprises most of the ordinary matter energy density in the universe. Astronomers have long known that antimatter doesn't exist naturally anywhere in the universe, but the SM predicts that the Big Bang should have produced an equal amount of matter and antimatter. That is, there is an asymmetry between the baryon density and antibaryon density. Since we don't know how this asymmetry occurred, when we model the baryon energy density, we set it in the initial conditions of the model. Since the dark matter energy density and baryon energy density are similar (within an order of magnitude), one might expect that the dark matter and baryons evolved in similar ways in the early universe. In that case, the dark matter energy density is also set by an asymmetry. This is the motivation for the proposal of ADM. In our model, leptogenesis creates an asymmetry in leptons [8], which through various interactions is transported to the baryons and dark matter. This creates the asymmetry in our initial conditions.

Conservation laws play an important role in physics. Each conservation law corresponds to a symmetry. Knowledge of these conservation laws tells us what processes can and cannot occur. One example of a conservation law is conserving particle number, which we would like to include in our model. Conventional models of ADM have only one dark matter flavor, which makes it easy to conserve the total number of dark matter particles, $n_{tot} = n_\chi - n_{\bar{\chi}}$, where χ denotes dark matter and $\bar{\chi}$ denotes antidark matter. By contrast, our model has three flavors, called e, μ, and τ. We want to retain the conservation of total dark matter number, but now $n_\chi = n_{\chi_e} + n_{\chi_\mu} + n_{\chi_\tau}$ and $n_{\bar{\chi}} = n_{\bar{\chi}_e} + n_{\bar{\chi}_\mu} + n_{\bar{\chi}_\tau}$. Fortunately, n_{tot} can still be conserved, and the interactions that conserve them are covered in the next section.

2 Background

2.1 Interactions

There are two types of interactions that we considered in the SADM model.

2.1.1 Flavored Dark Matter

The flavored dark matter (FDM) interactions are four interactions that involve multiple flavors of dark matter at once [9]. These are the interactions that generated the asymmetry in the initial conditions by transferring it from the leptons. Over the time period that our equations are being solved, they serve to redistribute the asymmetries in one flavor to another.

First we consider the process (called diagram 2, for historical reasons) that takes a dark matter particle of flavor i, χ_i, and collides it with a antidark matter particle of flavor j, $\bar{\chi}_j$, where $i, j \in \{e, \mu, \tau\}$. In this collision, a lepton of flavor i, l_i, and an antilepton of flavor j, $\bar{l}_j$, are created. Symbolically we represent this as $\chi_i \bar{\chi}_j \to l_i \bar{l}_j$. A measure of how likely the process is to occur is the cross section σ. Strictly speaking, σ is the area within which two particles must meet for scattering to take place [10]. This interaction is much more likely to occur if there are large amounts of χ_i and $\bar{\chi}_j$, since the two will be more likely to come into contact, but this is not encoded in σ. This is encoded in the Boltzmann equations. For diagram 2,

$$\sigma_{ij}^2 = \frac{\lambda^2}{128\pi} \frac{(m_{\chi_i} + m_{\chi_j})^2}{m_\phi^4}. \tag{1}$$

Here, λ is called the coupling and corresponds to the strength of the interaction. It is not a measurable quantity, but we can change its value and see how that affects the dark matter evolution. The value m represents the mass of the subscript particle. The particle ϕ is a scalar particle that mediates the interaction. Its mass is much larger than the χ mass.

Diagram 3 is the process $\chi_i \bar{l}_i \to \bar{\chi}_j \bar{l}_j$. To a first approximation, the condition that the

cross section be nonzero is $C_{ij}(T) \equiv m_{\chi_i}^2 - m_{\chi_j}^2 + 2m_{\chi_i}T > 0$. The cross section is

$$\sigma_{ij}^3 = \begin{cases} \dfrac{\lambda^4}{64\pi} \dfrac{C_{ij}(T)^2}{m_{\chi_i}(m_{\chi_i}+T)(m_{\chi_i}^2 - m_\phi^2 + 2m_{\chi_i}T)^2} & C_{ij}(T) > 0 \\ 0 & \text{otherwise} \end{cases}. \tag{2}$$

Time flows backwards in the $-T$ direction since temperature decreases as the universe expands, and we note that the interaction proceeding from higher mass to lower mass has a larger probability of happening at later times. The smaller the mass gap, the later the process is relevant. We can see this directly by examining $C_{ij}(T)$. In the limit of a small mass gap $\Delta m = m_{\chi_j} - m_{\chi_i}$, $C_{ij}(T) = m_{\chi_i}^2 - (\Delta m + m_{\chi_i})^2 + 2m_{\chi_i}T \approx 2m_{\chi_i}(T - \Delta m)$. Thus the process is relevant until the universe cools below $T \approx \Delta m$.

Diagram 4 is the process $\chi_i \to \chi_j l_i \bar{l}_j$, i.e., the decay from one flavor to another. In order for the decay to happen, because of energy conservation, the decays can only flow from a heavy flavor to a light flavor. The cross section is

$$\begin{aligned} \sigma_{ij}^4 =& \frac{\lambda^4}{6144\pi^3} \frac{1}{m_{\chi_i}^3 m_\phi^4} \\ & \times \left(m_{\chi_i}^8 - m_{\chi_j}^8 - 8m_{\chi_i}^6 m_{\chi_j}^2 + 8m_{\chi_i}^2 m_{\chi_j}^6 + 12 m_{\chi_i}^4 m_{\chi_j}^4 \log \frac{m_{\chi_i}^2}{m_{\chi_j}^2} \right). \end{aligned} \tag{3}$$

In the long term, the decays will transfer all of the dark matter energy density into the lowest mass flavor.

Diagram 5 is the process $\chi_i l_j \to \chi_j l_i$. The cross section is

$$\sigma_{ij}^5 = \begin{cases} \dfrac{\lambda^4}{384\pi} \dfrac{N_{ij}(T)}{m_{\chi_i}^2 m_\phi^4 (m_{\chi_i}+T)(m_{\chi_i}+2T)^2} & C_{ij}(T) > 0 \\ 0 & \text{otherwise} \end{cases}. \tag{4}$$

where the numerator $N_{ij}(T) = C_{ij}(T)^2(3m_{\chi_i}^3 + 3m_{\chi_i}m_{\chi_j}^2 + 10m_{\chi_i}^2 T + 2m_{\chi_j}^2 T + 8m_{\chi_i}T^2)$.

2.1.2 Z prime

The photon is the electromagnetic "force-carrier," that is, it mediates interactions between the charged particles of everyday matter. Similarly, the Z' (Z prime, or dark photon) is a hypothetical particle that mediates a force similar to electromagnetism between "dark charged" dark matter particles. We know that dark matter is not electromagnetically charged because we cannot see it, so it doesn't interact with photons. But it is possible that dark matter has its own kind of charge, dubbed dark charge, that allows this Z' particle to interact with it. If we add this force to the SADM theory, there is another kind of interaction to consider, the process $\chi_i\bar{\chi}_i \to Z'Z'$. The cross section

$$\sigma^{Z'} = \frac{\alpha_D^2\pi}{m_{\chi_i}^2}. \tag{5}$$

The Z' interaction serves to simply decrease the overall number of dark matter particles in the universe, as they turn into dark photons. This interaction has a different coupling than FDM, called α_D. With two different couplings, interesting phenomenological consequences can occur. In section 3 we will explore the possibilities $\lambda \gg \alpha_D$, $\lambda \approx \alpha_D$, and $\lambda \ll \alpha_D$.

2.2 Boltzmann equations

Writing down the closed form behavior of a system that is not in thermal equilibrium is extremely difficult or impossible. It is described by a differential equation known as a Boltzmann equation. In general, this is applicable to our situation because as the universe expands, it cools, and various particles fall out of equilibrium with the universe. For the SADM case, there are 6 Boltzmann equations, one for each particle $p \in \{\chi_e, \chi_\mu, \chi_\tau, \bar{\chi}_e, \bar{\chi}_\mu, \bar{\chi}_\tau\}$. The SADM Boltzmann equations are nonlinear, coupled, and impossible to solve by hand. For the one-flavor case, there are approximate analytical solutions, but the three-flavor case must be solved numerically.

The general equation for the flavor i interacting with flavors $j, k \neq i$ is as follows:

$$
\begin{aligned}
\frac{m_{\chi_e}^2 g_s^{\frac{1}{2}}}{.602 x m_{Pl}} \frac{dn_{\chi_i}}{dx} = & \\
& - \frac{5}{x^3} \frac{m_{\chi_e}^2 g_s^{\frac{1}{2}}}{m_{Pl}} n_{\chi_i} \\
& - \sigma_{ii}^2 \left(n_{\chi_i} n_{\bar{\chi}_i} - n_{\chi_i, eq} n_{\bar{\chi}_i, eq} \right) \\
& - \sigma_{ij}^2 \left(n_{\chi_i} n_{\bar{\chi}_j} - n_{\chi_i, eq} n_{\bar{\chi}_j, eq} \right) \\
& - \sigma_{ik}^2 \left(n_{\chi_i} n_{\bar{\chi}_k} - n_{\chi_i, eq} n_{\bar{\chi}_k, eq} \right) \\
& - \sigma_{ij}^3 \left(n_{\chi_i} - \frac{n_{\chi_i, eq} n_{\chi_j}}{n_{\chi_j, eq}} \right) n_{\bar{l}_i, eq} \\
& - \sigma_{ik}^3 \left(n_{\chi_i} - \frac{n_{\chi_i, eq} n_{\chi_k}}{n_{\chi_k, eq}} \right) n_{\bar{l}_i, eq} \\
& - \sigma_{ij}^5 \left(n_{\chi_i} - \frac{n_{\chi_i, eq} n_{\chi_j}}{n_{\chi_j, eq}} \right) n_{l_j, eq} \\
& - \sigma_{ik}^5 \left(n_{\chi_i} - \frac{n_{\chi_i, eq} n_{\chi_k}}{n_{\chi_k, eq}} \right) n_{l_k, eq} \\
& - \begin{cases} \sigma_{ij}^4 \left(n_{\chi_i} - \frac{n_{\chi_i, eq} n_{\chi_j}}{n_{\chi_j, eq}} \right) & m_{\chi_i} > m_{\chi_j} \\ (-1) \sigma_{ji}^4 \left(n_{\chi_j} - \frac{n_{\chi_j, eq} n_{\chi_i}}{n_{\chi_i, eq}} \right) & m_{\chi_i} < m_{\chi_j} \\ 0 & m_{\chi_i} = m_{\chi_j} \end{cases} \\
& - \begin{cases} \sigma_{ik}^4 \left(n_{\chi_i} - \frac{n_{\chi_i, eq} n_{\chi_k}}{n_{\chi_k, eq}} \right) & m_{\chi_i} > m_{\chi_k} \\ (-1) \sigma_{ki}^4 \left(n_{\chi_k} - \frac{n_{\chi_k, eq} n_{\chi_i}}{n_{\chi_i, eq}} \right) & m_{\chi_i} < m_{\chi_k} \\ 0 & m_{\chi_i} = m_{\chi_k} \end{cases} \\
& - \sigma^{Z'} \left(n_{\chi_i} n_{\bar{\chi}_i} - n_{\chi_i, eq} n_{\bar{\chi}_i, eq} \right),
\end{aligned}
\tag{6}
$$

where $g_s = 90$ is the number of relativistic degrees of freedom, $m_{Pl} = 1.22 \times 10^{19}$ is the Planck mass, and n_p is the number density of the particle p (this is how the fact that particles will be more likely to interact if their densities are larger is encoded into the Boltzmann equation). The equation is parametrized by a variable $x = \frac{m_{\chi_e}}{T}$, which increases with time.

The parametrization has the advantage that the e flavor becomes nonrelativistic at $x = 1$. To obtain the equation for flavors j or k, just permute the indices as $i \to j \to k \to i$ once or twice, respectively. To obtain the equation for the antimatter, $n_p \leftrightarrow n_{\bar{p}}$ for each particle p.

The first term on the right-hand side is the Hubble term, and accounts for the expansion of the universe. The next three terms are the terms that account for the diagram 2 interactions between flavors i and i, i and j, and i and k, respectively. The σ_3 terms describe the diagram 3 interactions between i and j and i and k. The σ_5 terms do the same for diagram 5. The σ_4 terms are piecewise in dark matter mass to account for the dark matter decays from higher mass to lower mass. The final term describes dark matter annihilation into two Z' particles.

2.3 Cosmology and Thermodynamics

2.3.1 Chemical Potential

The chemical potential μ, roughly, is the amount of energy you add to a system by adding a particle. This is relevant in situations in which particle interactions are happening because the numbers and types are particles are being changed. Consider a particle interaction $i + j \leftrightarrow k + l$. If the reaction is in chemical equilibrium, we have the equation

$$\mu_i + \mu_j = \mu_k + \mu_l \tag{7}$$

. Given the chemical potential, in the non-relativistic limit [11], we have

$$n_{p,eq} = g \left(\frac{m_p T}{2\pi} \right)^{3/2} \exp\left(-\frac{m_p - \mu_p}{T} \right), \tag{8}$$

where n_p is the number density of particle p and g is the number of internal degrees of freedom of the particle. For the spin-$1/2$ particles that we will deal with, $g = 2$. In the SADM model, if FDM interactions are out of equilibrium and nonrelativistic, then the asymmetry between

particle and antiparticle $n_p - n_{\bar{p}}$ is some fixed value ΔY, and we find

$$\mu_p = T \operatorname{arctanh}\left(\frac{\Delta Y \exp\left(\frac{m}{T}\right)}{2g\left(\frac{mT}{2\pi}\right)^{3/2}}\right). \tag{9}$$

In general, the calculation will not be so simple and will have to be completed numerically by solving the equations derived from chemical equilibrium considerations (7).

2.3.2 Expansion of the Universe

We've known since the early 1900s that the universe is expanding. Mathematically, we say that if the distance between two points today is d_0, then at any time t the distance is $d(t) = a(t)d_0$, where $a(t)$ is known as the scale factor, the ratio of distances at time t to distances today [12]. We see that $a(today) = 1$. We use the Hubble parameter $H = \frac{\dot{a}(t)}{a(t)}$ as a measure of the expansion rate; today's value is 67 $\frac{\text{km/s}}{\text{Mpc}}$, meaning that galaxies 1 Mpc from the Earth are moving away from us at a speed of 67 km/s. This gives us a rate at which to compare other astrophysical rates during calculations.

Because of this expansion, an important concept is the comoving volume. Consider some volume V in space. As the universe expands, the volume V will enlarge to $a^3(t)V$. Considering the comoving volume means your frame of reference expands at the same rate, so the volume remains constant in your frame. Because the volume is expanding, the temperature of the universe must decrease, and we find that

$$a(t) \propto \frac{1}{T(t)}. \tag{10}$$

This is how we know that temperature decreases as time passes. Assuming the particle is in thermal equilibrium with the universe, we can use relativistic approximations when $m < T$ and nonrelativistic approximations when $m > T$.

2.3.3 Comoving Number Densities

To solve the Boltzmann equation, we need to find the number densities in a comoving frame $Y_{p,eq}$ of a particle p. Let the reaction rates of particles in the early universe be denoted Γ_{int}. It turns out that $\Gamma_{int} > H$. This implies that the entropy per comoving volume S is constant [11]. In order to find the comoving number density Y_p, we define the entropy density

$$s = \frac{S}{V} = \frac{2\pi^2}{45} g_s T^3. \tag{11}$$

Then simply $Y_p = \frac{n_p}{s}$. Then for nonrelativistic particles in thermal equilibrium we have

$$Y_{p,eq} = \frac{45g}{4\sqrt{2}\pi^5 g_s} \left(\frac{m}{T}\right)^{\frac{3}{2}} \exp\left(-\frac{m-\mu}{T}\right) \tag{12}$$

2.3.4 Leptogenesis

The observation that the universe has more matter than antimatter has motivated the theory of leptogenesis. Leptogenesis provides an explanation for this phenomenon by suggesting that interactions just after the Big Bang produced an asymmetry between leptons and antileptons, so that the density of leptons became much greater than the density of antileptons. After this asymmetry is generated it is conserved because no SM interactions violate lepton number. In the context of SADM, we assume there is some initial asymmetry Δ_i in the leptons l_i, which is transferred to the dark matter by FDM interactions and to the baryons by SM interactions. This leaves us with the asymmetry that we see today.

2.3.5 Freeze Out

The thermal behavior of particles relies on the ratio between Γ_{int} and H. When $\Gamma_{int} > H$, enough interaction is occurring that the particle stays in thermal equilibrium. In order to fall out of equilibrium, the interaction rate for some process must fall below H [11]. We call this process freezing out and say the x value at which it happens is x_F. Once $\Gamma_{int} < H$, then the

reaction is frozen out. When a reaction freezes out, n will start to diverge from n_{eq}. After a long time, n will stabilize and reach its freeze out value n_F. This value is proportional to the relic density

$$\Omega_\chi h^2 = 2.755 \times 10^8 \frac{m}{\text{GeV}} \frac{n_F}{s_F}, \tag{13}$$

which is the density the particle asymptotes to after freeze out.

The FDM interaction falls out of equilibrium at a very high temperature where the dark matter is relativistic. Then the initial asymmetry values in each dark matter flavor ΔY_i are

$$\begin{bmatrix} \Delta Y_e \\ \Delta Y_\mu \\ \Delta Y_\tau \end{bmatrix} = \frac{2}{15} \begin{bmatrix} -2 & 1 & 1 \\ 1 & -2 & 1 \\ 1 & 1 & -2 \end{bmatrix} \begin{bmatrix} \Delta_e \\ \Delta_\mu \\ \Delta_\tau \end{bmatrix}. \tag{14}$$

We now make a distinction between the symmetric and asymmetric component of the dark matter. Because of the asymmetry, there will be either more dark matter or more antidark matter. Without loss of generality, say there is more dark matter. For each antidark matter particle, assign it a corresponding dark matter particle. The asymmetric component is the portion of dark matter particles that do not have an corresponding antiparticle, $n_{AS} = n_\chi - n_{\bar{\chi}}$. The symmetric component are the particles with partners, $n_S = n_{tot} - n_{AS} = 2n_{\bar{\chi}}$. Then $n_{tot} = n_S + n_{AS}$ as necessary.

The Z' interaction, at large enough α_D, serves to annihilate the symmetric component because each particle will interact with an antiparticle with high probability. Assuming this is accomplished, the asymmetry values (14) are simply the dark matter number densities today.

3 Program Overview

I wrote a program in Mathematica 11.0 that numerically solves the SADM Boltzmann equation (6). With the solutions, we can examine in detail how the FDM and Z' interactions

affect the evolution of the dark matter density, its symmetric and asymmetric components, and their relic densities.

3.1 Chemical Potentials

In order to solve the equation, we must first find the chemical potentials for the dark matter, μ_{χ_i}. We originally thought that we would need to consider the relativistic regime $x < 1$, but at least for immediate phenomenological purposes that regime is unnecessary because n will track n_{eq} until freeze out much later than $x = 1$ anyway. Unfortunately for us, the nonrelativistic chemical potential is the difficult one to calculate in general.

If the dark matter is not in equilibrium with the FDM interactions (for example, if it is equilibrium with the Z' interaction), this is simply (8). However, if it is, we must numerically solve for them using the chemical equilibrium constraints provided by the SM and FDM interactions. Simplifying these equations gives four unknowns, μ_{χ_e}, μ_{χ_μ}, μ_{χ_τ}, and μ_ϕ. Using the constraints $\Delta_i = \frac{B}{3} - L_i$ where B and L are the net baryon and lepton numbers and $\sum_i n_{\chi_i} = n_\phi$, it's possible to get a solution. There is no closed form solution due to the combination of exponentials and polynomials, so the solution must be found numerically at specific x. We use `FindRoot` to solve the equations from $x = 1$ to $x = 100$ in intervals of .01 at 50-digit precision (any less is too low to distinguish global and local minima). `FindRoot[eqn1, eqn2, ...}, {{x, x0}, {y, y0}, ...}]` searches for a numerical solution to the simultaneous equations eqn_i. For a typical value of $m_{\chi_e} \approx 100$ GeV, this corresponds to $T = 10^{15}$ to 10^{13} K or approximately $t = 10^{-10}$ to 10^{-7} s after the Big Bang, so this is well after leptogenesis but before nucleosynthesis. This range is appropriate because it covers typical values of freeze out time $x \approx 20$, so results show tracking of n_{eq} to decoupling to approaching n_F. We obtain with a discrete set of points $\{\mu_{\chi_i}(1),\ \mu_{\chi_i}(1.01),\ \ldots,\ \mu_{\chi_i}(100)\}$ and use `Interpolation` approximate the correct continuous μ. This outputs the chemical potentials in a form suitable for numerical solving, since the step sizes taken by Mathematica to solve the Boltzmann equation may not be as uniform as the size selected for finding μ.

The lepton potentials are then linear combinations of the form

$$\mu_{l_i} = \frac{1}{12}\left(9\mu_\phi + 8\mu_{\chi_i} - 4\sum_{j\neq i}\mu_{\chi_j}\right). \tag{15}$$

3.2 Obtaining Solutions

With an expression for the dark matter and lepton chemical potentials, we can now solve the Boltzmann equations. The initial conditions imposed are $n_{\chi_i}(x = x_{start}) = n_{\chi_i,eq}(x = x_{start})$. The initial conditions contain an implicit assumption that no particle is frozen out earlier than x_{start}, because $n(x) \neq n_{eq}(x)$ for any $x > x_F$. We must check this. In practice, it simply requires a visual scan that n tracks n_{eq} around x_{start} in the outputted plots. If $x_F < x_{start}$, x_{start} can be moved as early as 1. However, obtaining the solution is quicker the later x_{start} is, and since n tracks n_{eq} until x_F anyway, a typical value would be $x_{start} \approx 15$.

To obtain the solution we use `ParametricNDSolveValue`, Mathematica's differential equation solver. Formally, `ParametricNDSolveValue[eqns, expr, {x,x`$_{\texttt{min}}$`,x`$_{\texttt{max}}$`}, pars]` returns the value of *expr* with functions determined by a numerical solution to the ordinary differential equations *eqns* with the independent variable x in the range x_{min} to x_{max} with parameters *pars*. To *eqns* we input the 6 Boltzmann equations corresponding to each particle $p \in \{\chi_e, \chi_\mu, \chi_\tau, \bar{\chi}_e, \bar{\chi}_\mu, \bar{\chi}_\tau\}$ along with the initial conditions; to *expr* we input the 6 number densities n_p we want to find; to *pars* we input the parameters, usually some of $\{\lambda, \alpha_D$, masses, or asymmetries$\}$.

A major struggle in obtaining accurate solutions was the fact that the SADM Boltzmann equation is stiff, that is, the step size must be extremely small to avoid numerical instability. Otherwise, the numerical solutions will diverge from the true solution. In many cases Mathematica was not able to take a small enough step size to account for this stiffness. In order to solve this problem, we were able to change two parameters, the precision and method used to solve the equation. To some extent, `ParametricNDSolveValue` is a black box, but it does allow you a few options like this. We required the solutions to have a 20-digit preci-

sion. Then, depending on the exact parameters chosen, used different methods to solve the differential equation. In particular, for large λ, using `Method → BDF` was effective. Unlike Euler's method that uses only the previous point and derivative to determine the value of the solution at the next point, `BDF` uses a linear combination of several previous points to determine the next solution value. It is a well-known method for solving stiff differential equations. For worse stiffness, `Method → StiffnessSwitching` was effective. However, this option was not ideal in most cases. `StiffnessSwitching` will instruct Mathematica to switch between methods designed for stiff and nonstiff equations. At each step, Mathematica checks if the equation is stiff, and if so, switches to the stiff solver. This stiff solver will use incredibly small step sizes and solving the entire equation can take a prohibitively long time. When using `StiffnessSwitching` it was especially helpful to define x_{start} as close to x_F as possible to speed up the calculation.

The output is 6 functions n_p, the number density of each particle as the universe expands. In the following section, we have plotted the comoving number density Y_p. If we are interested in the time-evolution of the dark matter, it is useful to plot the functions over the whole range $x_{start} \leq x \leq 100$. This helps interpret the effects of the FDM and Z' interactions. From a phenomenological standpoint, more useful is scanning over some set of parameter space and plotting the asymmetric component relic density. Interesting values to scan over include λ, α_D, or the χ masses.

4 Discussion

In this section we interpret the solutions to the SADM Boltzmann equation at various parameter points and how the results change as we vary initial parameters. For the following discussion we restrict ourselves to the simplest lepton asymmetry possible, $\Delta_e = 10^{-11}$, $\Delta_\mu = 0 = \Delta_\tau$.

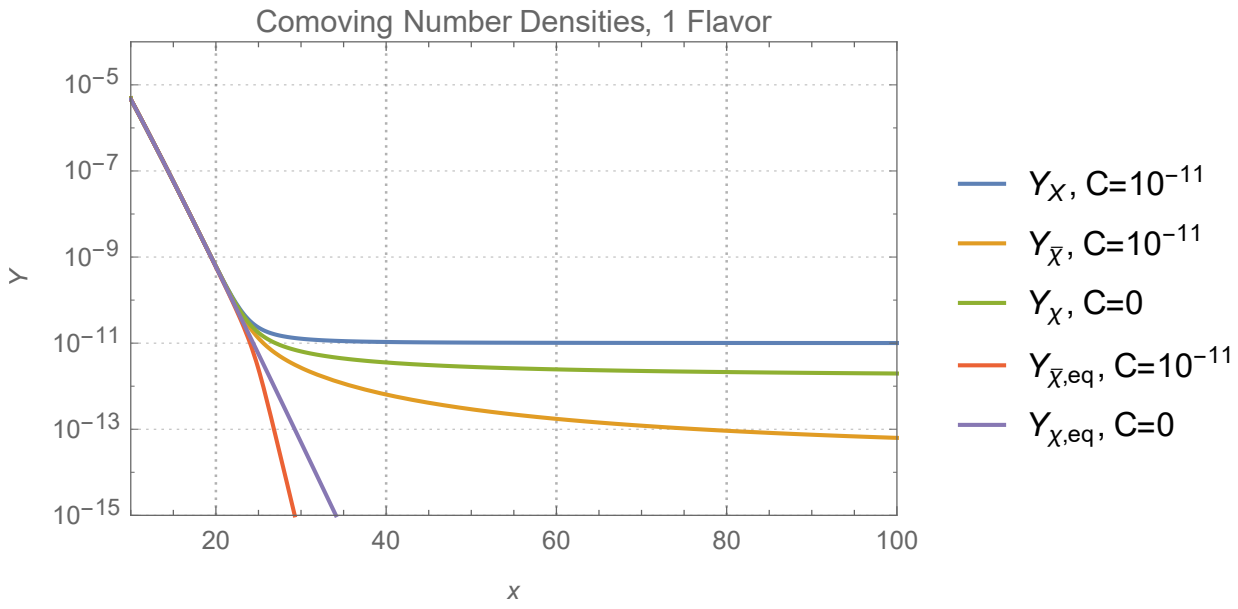

Figure 1: Comoving number densities are plotted for the 1-flavor case.

4.1 One-Flavor Case

Analysis of the one-flavor case [13] is the easiest way to get a handle on what type of solution we should be expecting. Effectively, since the only interaction possibility is $\chi\bar{\chi}$ annihilation, this is the Z' interaction with no FDM.

In Figure 1, we have plotted the comoving number densities as a function of x for symmetric ($C = 0$) and asymmetric ($C = 10^{-11}$) cases at the parameter point $m = 150$ GeV, where C is the initial asymmetry $n_\chi - n_{\bar{\chi}}$. In both cases, for small x, Y_p is essentially equal to $Y_{p,eq}$, and the freeze out value $x_F \approx 23$. For the symmetric case, at $x > x_F$, the annihilations are no longer happening fast enough to overcome expansion of the universe, and the abundance approaches its final value quickly. For the asymmetric case, at $x > x_F$, the χ density is constrained to be greater than C, and it asymptotically approaches this value as each individual particle is less and less likely to meet and annihilate with an antiparticle $\bar{\chi}$. On the other hand, the $\bar{\chi}$ density can be arbitrarily low, and continues to deplete significant fractions for a long time.

4.2 FDM Interaction Only

The case of including only the FDM interaction terms in the Boltzmann equation with all three flavors is much more interesting than the simple one-flavor case. The solution to the FDM Boltzmann equation is given in Figure 2 at the parameter point $(m_e, m_\mu, m_\tau) = (150\text{ GeV}, 150\text{ GeV}, 100\text{ GeV})$ and $\lambda = 1$, generated by `BDF`. Note the y-axes are not the same in each plot.

There are two essential differences from the one-flavor case. The first is that even though all flavors were given an initial asymmetry on the order of 10^{-11}, no flavor ends up with a significant asymmetry (the χ and $\bar{\chi}$ plots are lying on top of each other)—the e and μ densities are a factor of 10^{13} smaller than the original asymmetry at $x = 100$! This is due to the FDM annihilations and flavor mixing (diagrams 2, 3, and 5). As the flavors are redistributed, they will tend to turn particles with larger densities into particles with smaller densities due to the structure of the n_p terms in (6). This converts the asymmetric component into the symmetric component. The second difference is that the e and μ densities do not asymptote to some positive value in the lifetime of the simulation. This is due to diagram 4, the FDM decays. Because of the large e and μ mass compared to the τ mass, decays dominate the late-time functional form of the e and μ density. For $x_F < x \lesssim 40$, the density looks as if it may level off as in the one-flavor case. But as diagrams 3 and 5 become insignificant, the decays begin to dominate. By $x \approx 70$, e and μ flavors are effectively nonexistent, leaving the τ flavor as the lone dark matter particle. Note that the τ density is symmetric. So we truly have a secretly asymmetric mechanism at work here. In fact, the τ density curve looks very similar to the symmetric 1-flavor case with a larger relic abundance by a factor of 10.

To prove that the depletion of e and μ densities is due to FDM decays, I have plotted the densities in Figure 3 for the case that all flavors have degenerate mass $m = 150$ GeV. This effectively turns the decays off, and all densities asymptote to some positive relic density. Here it is plain that the decays caused this depletion.

Figure 4 shows that the FDM interactions have completely removed the asymmetry by

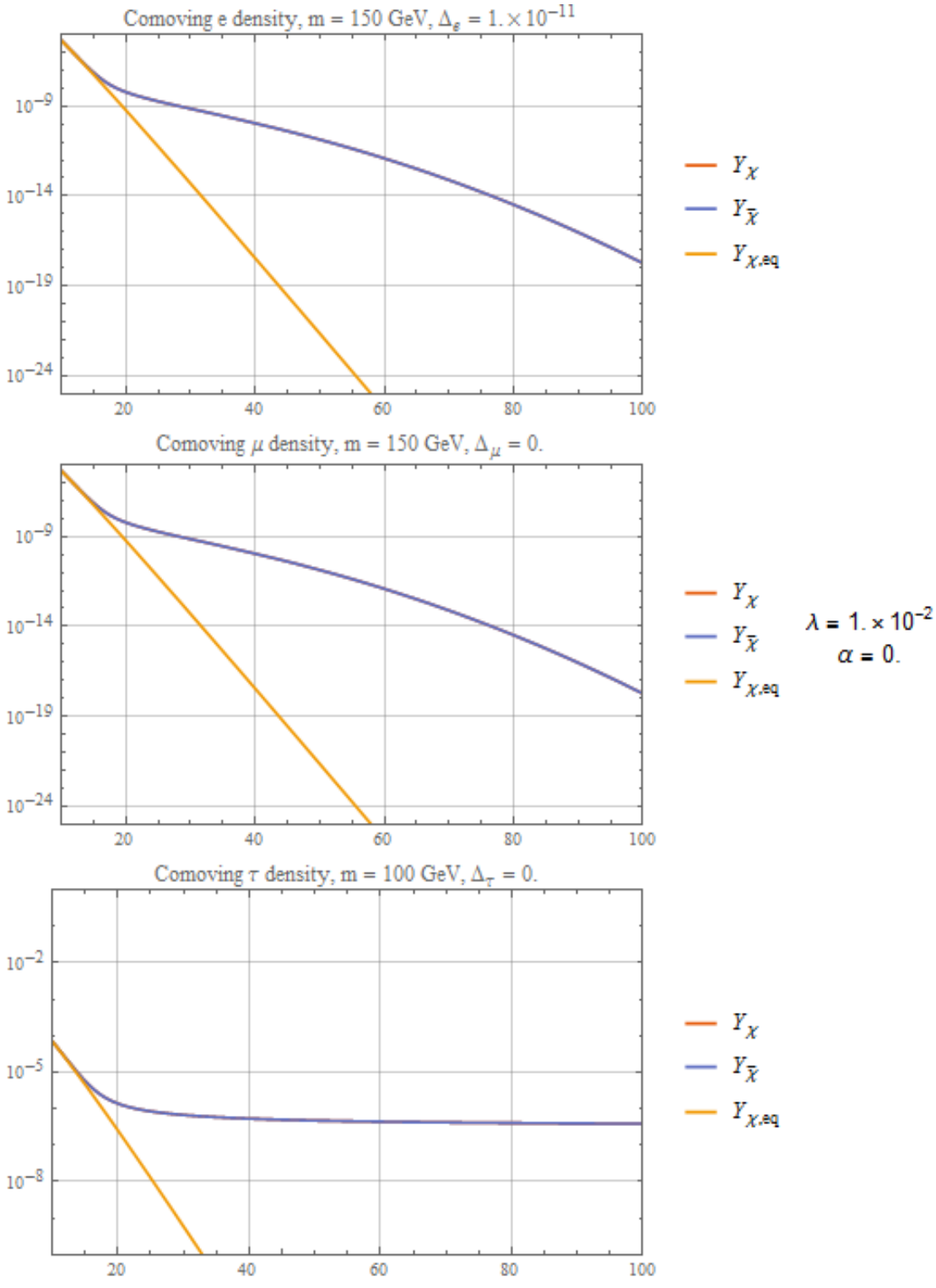

Figure 2: Comoving number densities are plotted for the FDM interactions.

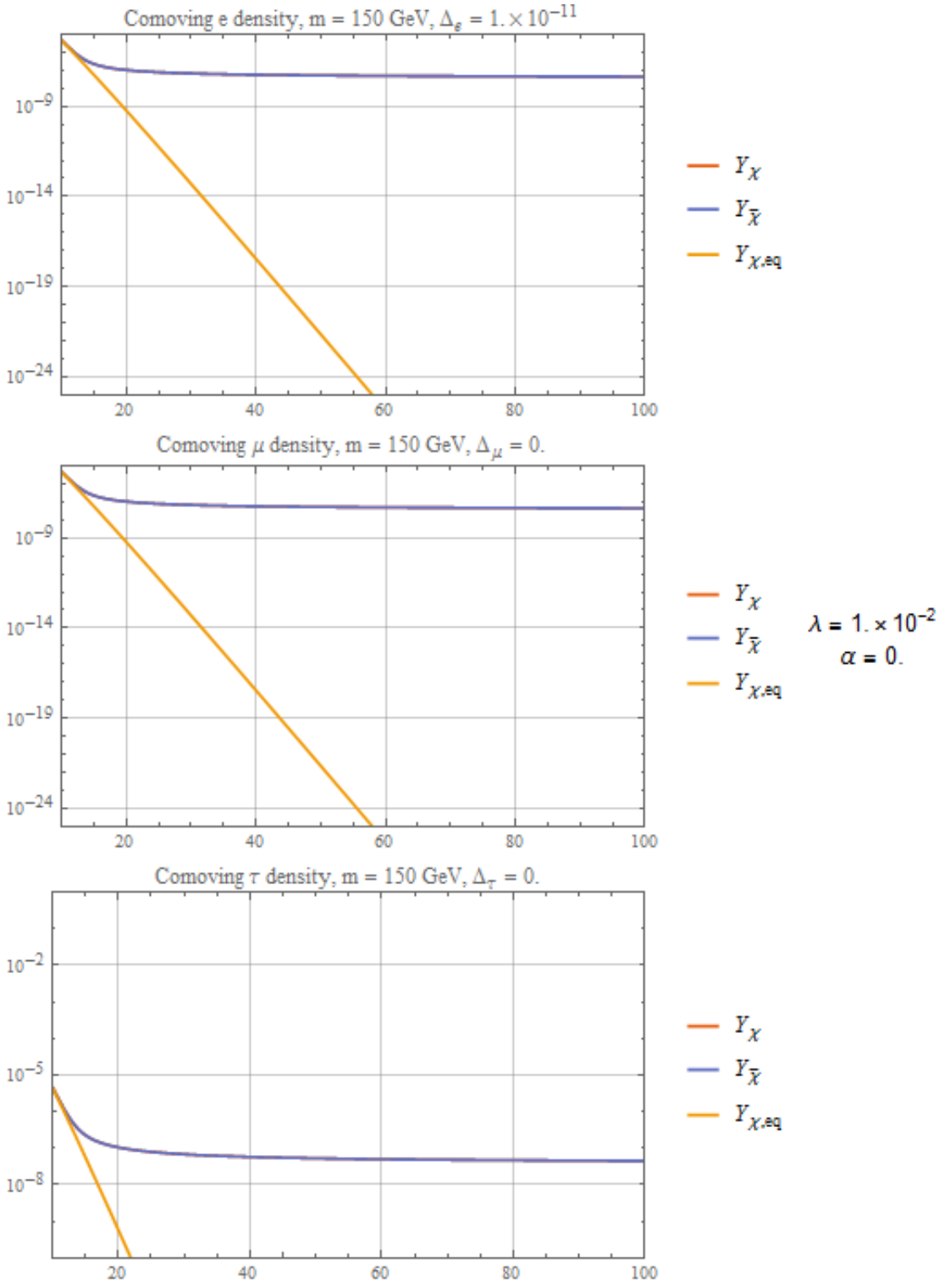

Figure 3: Comoving number densities are plotted for the FDM interactions when all flavors are degenerate.

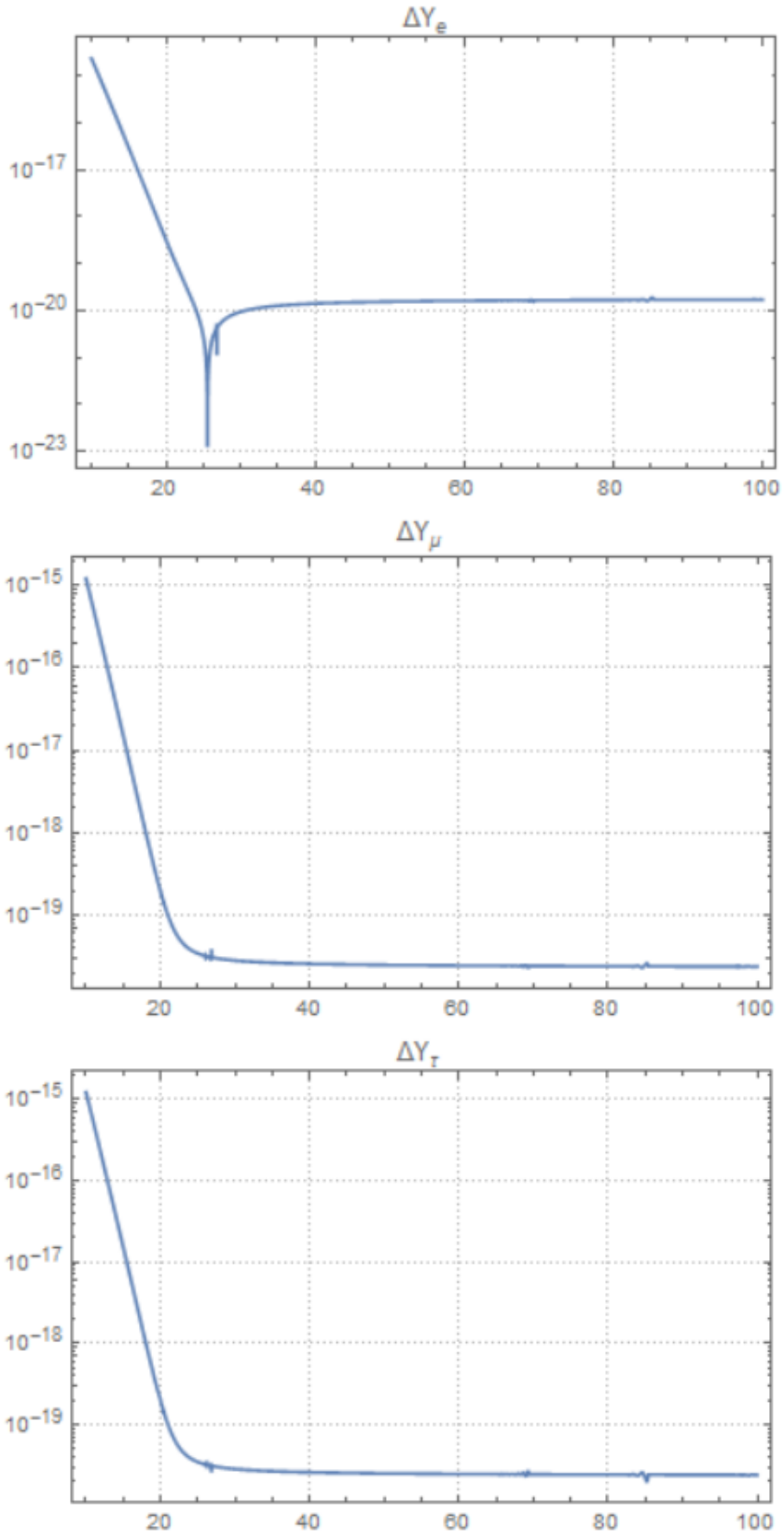

Figure 4: Asymmetry evolution is plotted for the FDM interactions.

$x \approx 30$. Note that although the graphs exhibit strange behavior afterwards, we have 20 digits of precision in our solutions, and so behavior around 10^{-20} is not an issue.

4.3 Full SADM Interactions

Here we return to the parameter point $(m_e, m_\mu, m_\tau) = (150 \text{ GeV}, 150 \text{ GeV}, 100 \text{ GeV})$. For this calculation, `BDF` was used. In Figure 5, we see the basic structure of the FDM interactions (asymmetry elimination, decays to lightest flavor). However, turning on the Z' interaction to a coupling $\alpha_D \approx \lambda$ has depleted the overall densities much more quickly than for $\alpha_D = 0$, and the relic density of τ is a factor of 10^6 smaller. We conclude that at this parameter point, the Z' interaction adds no new structure to the density evolution, merely suppresses it. However, the region $\lambda \neq 0 \neq \alpha_D$ is much broader than this one point. At this time, the program cannot overcome stiffness issues at parameter points that result in different evolution.

4.4 Z' Interaction Only

With FDM turned completely off $\lambda = 0$, so there is absolutely no communication between the flavors. In fact, this is nothing more than three copies of the one-flavor case running in the same universe. However, there is access to changing the coupling constant α_D, and the asymmetries are related by (14). The size of the coupling is of interest because we can then alter the amount of the symmetric component annihilated. To generate these solutions, `StiffnessSwitching` was used. At values of $\alpha_D > .1$, `BDF` was unable to overcome stiffness issues, while `StiffnessSwitching` was able to solve the equations.

In Figure 6, we have solved the Boltzmann equation ten times at various values of α_D. We plot the dark matter density fraction $\frac{n_\chi}{n_{tot}}$ at various values of α_D. We see that for $\alpha_D > 0.02$, the symmetric part of the dark matter density is completely annihilated $\left(\frac{n_\chi}{n_{tot}} \approx 0 \text{ or } 1\right)$. For $\frac{n_\chi}{n_{tot}} \approx 0$, $n_{\bar{\chi}}$ dominates the flavor; for $\frac{n_\chi}{n_{tot}} \approx 1$, n_χ dominates. Over a factor of 10 in

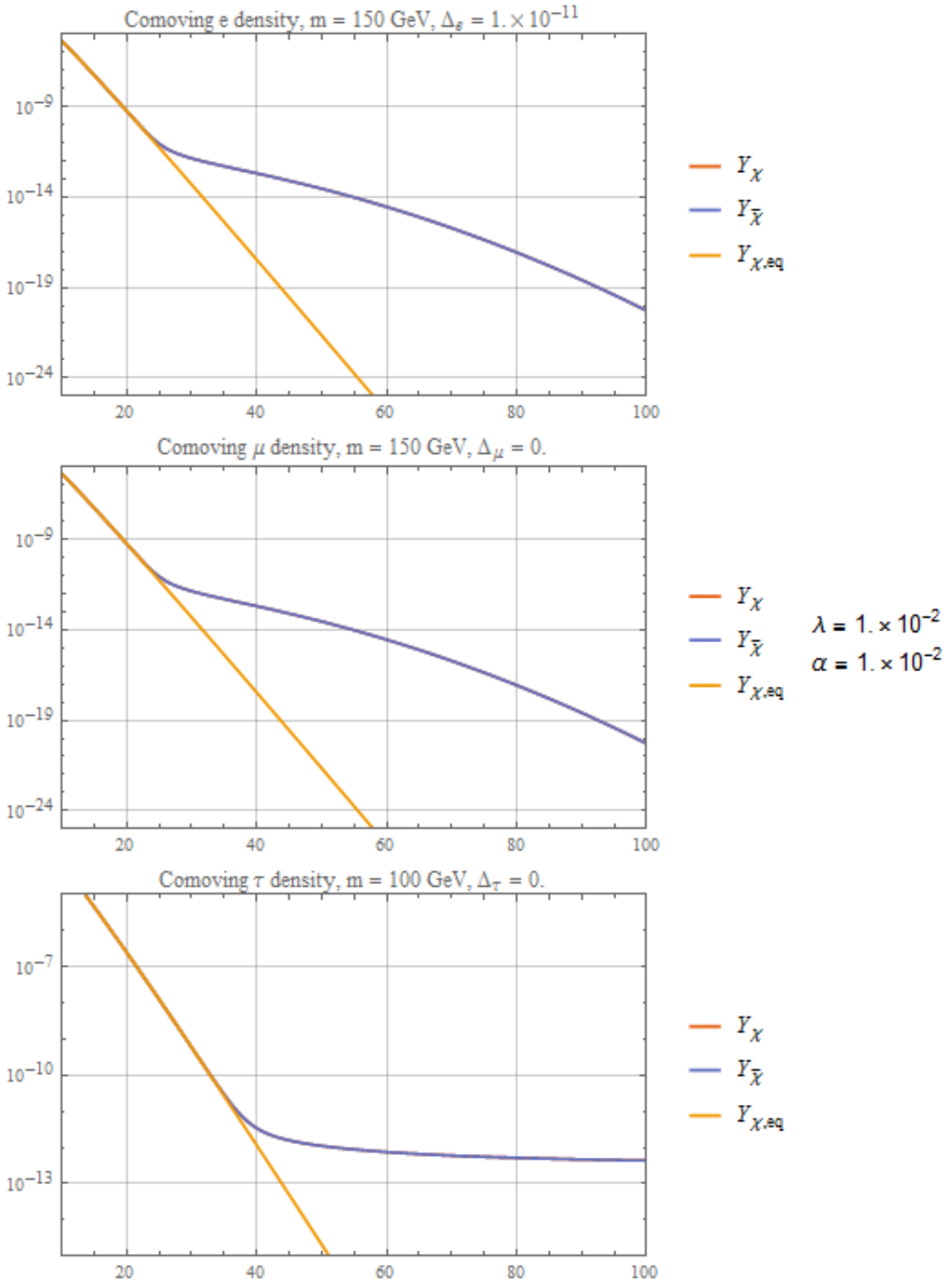

Figure 5: Comoving number densities are plotted for the full SADM interactions.

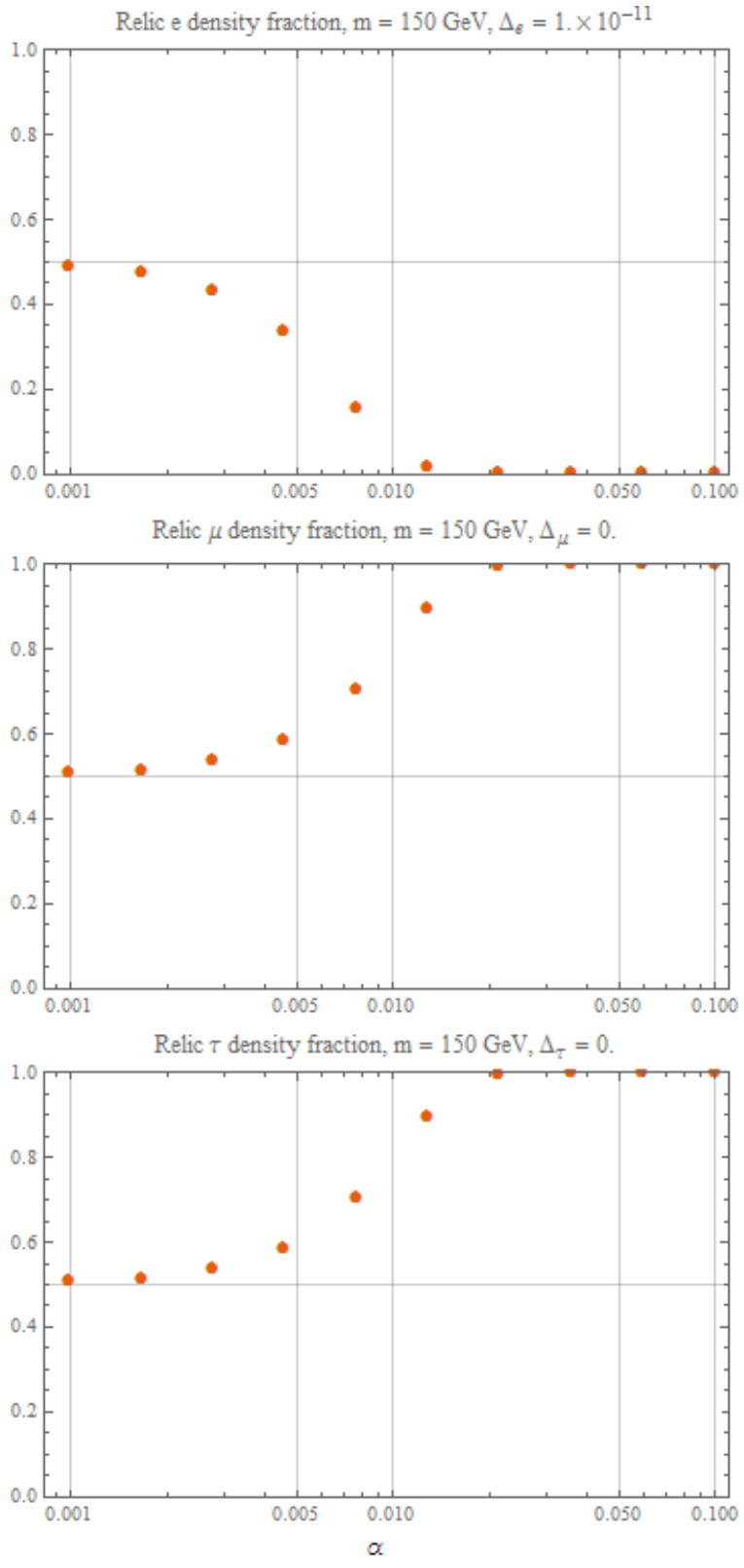

Figure 6: Dark matter density fractions are plotted for the Z' interaction.

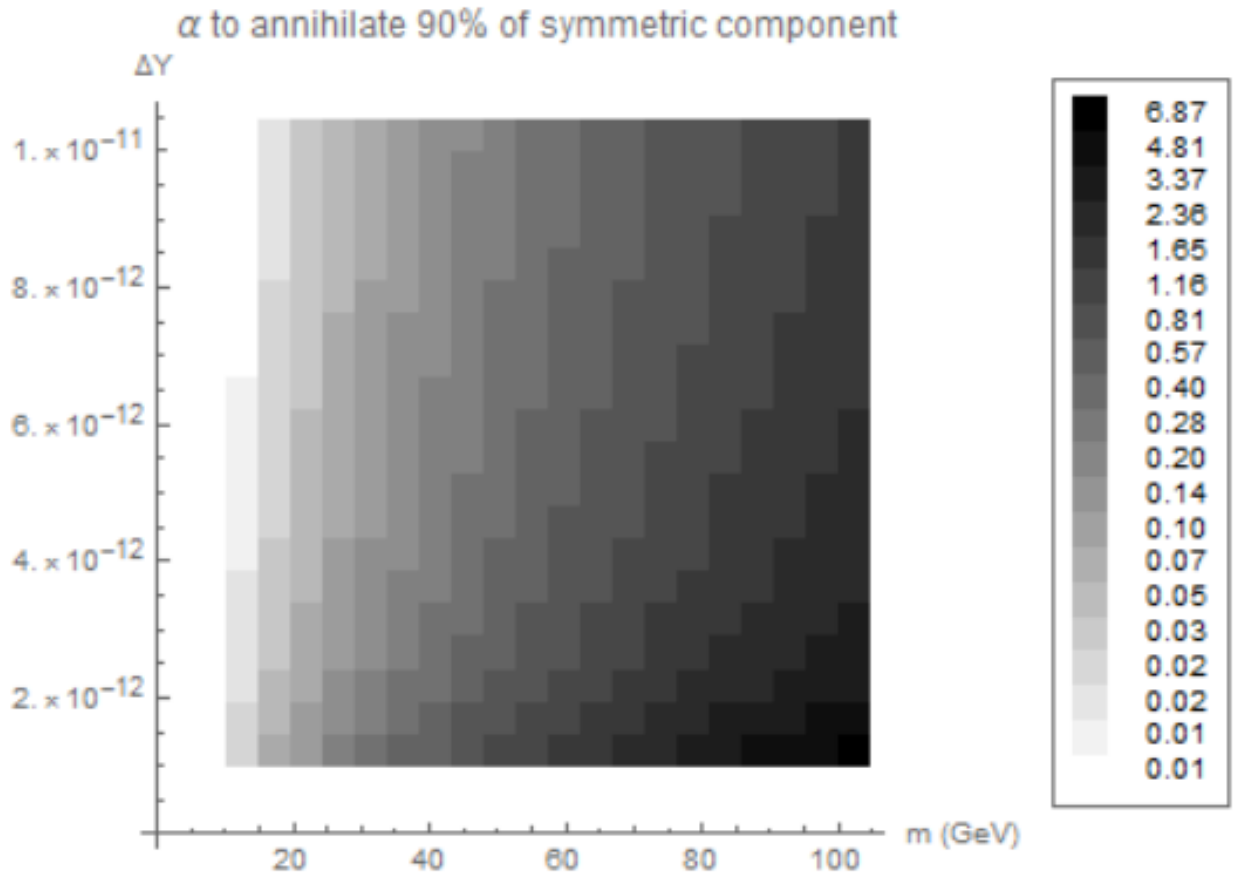

Figure 7: Dark matter density fractions are plotted for the Z' interaction.

α_D, the symmetric part falls from domination of the relic density to insignificance.

In Figure 7, we sampled 400 (m, Δ) parameter points and calculated the relic density fraction for multiple values of α_D. Then the points are colored according to the smallest α_D such that $\frac{n_\chi}{n_{tot}} > 0.9$ or < 0.1. We see that the larger the mass, the larger coupling required to annihilate the symmetric component. Over a factor of ten increase in mass, there is a factor of 300 increase in α_D. Since $\sigma^{Z'} \propto \frac{\alpha_D^2}{m^2}$, the cross section accounts for a factor of 10. The remaining factor of 30 can be explained by the fact that $n_{p,eq}$ decreases exponentially with m_p. We also see that increasing the initial asymmetry results in a smaller α_D needed to annihilate the symmetric component (clearly, because the asymmetric component is larger with larger initial asymmetry).

4.5 Future Goals

The Mathematica program has given us a basic insight into the structure of SADM theories with FDM and Z' interactions. There is still much interesting work to do in this regard. For example, it would be intriguing to examine how the number densities evolve under the FDM interaction in the limit of small and large mass splittings, particularly the effect on flavor mixing from diagrams 3 and 5 and how early the decays become relevant. Another route may be to probe the (λ, α_D) parameter space in regions where $\lambda < \alpha_D$ but the two interactions have similar size effects on n_p. In the current iteration of the differential equation solver the required values of λ are so small that the equation is stiff. It is possible that the solver can be refined or manually implemented in a way that is less sensitive to stiffness.

However, the immediate direction in which the program will be utilized will be to study the possibility that the dark matter forms bound states, i.e. dark atoms. In this model, based on [14], there is only a Z' interaction, and so the program is well-equipped to handle relevant numerical calculations. The Z' code calculates the number density of dark matter from equilibrium until the Z' interaction has become negligible. If the dark matter masses has a large (orders of magnitude) splitting, where one flavor is very light and oppositely charged ($\approx$ 1 MeV), then it is possible that the dark matter will combine to form dark atoms. These atoms would be similar to hydrogen in that there would be a light charged light particle bound to a heavy oppositely charged particle. Although it gives no information on how many particles should bind to form atoms, the code can help distinguish regions of parameter space that result in relic dark matter densities that are consistent with today's observations from regions that do not.

References

[1] E. Corbelli and P. Salucci, Mon. Not. Roy. Astron. Soc. 311 (2), (2000), arXiv:9909252 [astro-ph]

[2] X.-P. Wu, T. Chiueh, L.-Z. Fang and Y.-J. Xue, Mon. Not. Roy. Astron. Soc. 301 (3), (1998), arXiv:9808179 [astro-ph]

[3] G. Hinshaw, J. L. Weiland, R. S. Hill, N. Odegard, D. Larson, C. L. Bennett, J. Dunkley, B. Gold, M. R. Greason, N. Jarosik et al., ApJS 180 (2), (2009), arXiv:0803.0732 [astro-ph]

[4] S. Weinberg, Phys. Rev. Lett. 19 (1967)

[5] The ATLAS Collaboration, Phys. Rev. Lett. B716 (2012), arXiv:1207.7214 [hep-ex]

[6] S. M. Barr, Phys. Rev. D44, 3062 (1991)

[7] P. Agrawal, C. Kilic, S. Swaminathan, and C. Trendafilova, Phys. Rev. D95, 015031 (2017), arXiv:1608.04745 [hep-ph].

[8] M. Fukugita, Phys. Rev. B, B174 (1986)

[9] P. Agrawal, S. Blanchet, Z. Chacko and C. Kilic, Phys. Rev. D86, 055002 (2012), arXiv:1109.3516 [hep-ph]

[10] M. Peskin and D. Schroeder, *An Introduction to Quantum Field Theory* (Perseus Books, Reading, Mass., 1995).

[11] E. Kolb and M. Turner, *The Early Universe* (Addison-Wesley, Redwood City, Calif., 1990).

[12] C. W. Misner, K. S. Thorne, and J. A. Wheeler, *Gravitation* (W. H. Freeman, San Francisco, Calif., 1973).

[13] H. Iminniyaz, M. Drees, and X. Chen, JCAP 1107, 003 (2011), arXiv:1104.5548 [hep-ph].

[14] P. Agarawal, F.-Y. Cyr-Racine, L. Randall, and J. Scholtz, arXiv:1702.05482 [astro-ph.CO] (to be published).